

# Forward acceleration of the centre of mass during ski skating calculated from force and motion capture data

Caroline Göpfert<sup>1,2</sup> · Mikko V. Pohjola<sup>2</sup> · Vesa Linnamo<sup>2</sup> · Olli Ohtonen<sup>2</sup> · Walter Rapp<sup>3</sup> · Stefan J. Lindinger<sup>1</sup>

Published online: 20 December 2016

© The Author(s) 2016. This article is published with open access at Springerlink.com

**Abstract** The purpose of this paper was to present and evaluate a methodology to determine the contribution of bilateral leg and pole thrusts to forward acceleration of the centre of mass (COM) of cross-country skiers from multi-dimensional ground reaction forces and motion capture data. Nine highly skilled cross-country (XC) skiers performed leg skating and V2-alternate skating (V2A) under constant environmental conditions on snow, while ground reaction forces measured from ski bindings and poles and 3D motion with high-speed cameras were captured. COM acceleration determined from 3D motion analyses served as a reference and was compared to the results of the proposed methodology. The obtained values did not differ during the leg skating push-off, and force–time curves showed high similarity, with similarity coefficients (SC) >0.90 in the push-off and gliding phases. In V2A, leg and pole thrusts were shown to contribute 35.1 and 65.9% to the acceleration of the body, respectively. COM acceleration derived from ground reaction forces alone without considering the COM position overestimated the acceleration compared to data from motion analyses, with a mean difference of 17% ( $P < 0.05$ ) during leg push-off, although

the shapes of force–time curves were similar (SC = 0.93). The proposed methodology was shown to be appropriate for determining the acceleration of XC skiers during leg skating push-off from multi-dimensional ground reaction forces and the COM position. It was demonstrated that both the COM position and ground reaction forces are needed to find the source of acceleration.

**Keywords** Cross-country skiing · Propulsion · 3D motion analysis · System acceleration · Centre of mass

## 1 Introduction

Aided by various tools, human locomotion is highly versatile, allowing us to move effectively on dry land and snow, in and on water, and even through the air. During self-propelled locomotion, the propulsion (i.e. forces produced by the leg, trunk, and/or arms that lead to motion forward [1]) must be created by muscular force and transmitted to the environment in a manner that leads to movement in the desired direction. The particular form of propulsion is dependent on the environmental conditions [2].

On snow, cross-country (XC) skiing is a widespread recreational and competitive sport [3]. Good performance requires high energetic capacity and the ability to produce considerable propulsion effectively and economically [4, 5], while forces are transmitted to the ground through skis and poles when using different techniques. The propulsive force of XC skiing has been defined as the component of the three-dimensional (3D) resultant reaction force from each pole and/or ski in a forward direction acting on the skier [6]. There are two approaches to studying this force component.

✉ Caroline Göpfert  
caroline.goepfert@stud.sbg.ac.at

<sup>1</sup> Department of Sport Science and Kinesiology, University of Salzburg, Schlossallee 49, Hallein/Rif, 5400 Salzburg, Austria

<sup>2</sup> Sports Technology Unit, Department of Biology of Physical Activity, Neuromuscular Research Centre, University of Jyväskylä, Kidekuja 2, Snowpolis, 88610 Vuokatti, Finland

<sup>3</sup> Department of Sport and Sport Science, University of Freiburg, Schwarzwaldstraße 175, 79117 Freiburg im Breisgau, Germany

First, in several earlier studies, the horizontal propulsive ski and pole forces produced during classic skiing (e.g. [7–9]) and skating (e.g. [10]) were measured directly by two-dimensional (2D) or 3D force platforms placed in or under the snow. More recently, models for calculating the propulsive components from ground reaction forces (GRFs) and 3D kinematics measured with improved and miniaturized systems during roller ski skating [11–14] were developed. With this approach, the share of the resultant GRF pointing in the desired skiing direction was calculated by taking into account the ski orientation, ski edging angle, and track incline and the corresponding pole angles (e.g. [6, 11, 15, 16]). Now, more diverse questions have been posed regarding propulsive forces in XC skiing. Aspects that have been addressed include quantification of and discrimination between the contributions of the right and left poles and legs (e.g. [15, 17, 18]), comparison of techniques [19, 20], investigation of the mechanisms of speed, incline, or fatigue adaptations (e.g. [21–25]), or estimation of the effects by using innovative XC skiing equipment (e.g. [26–30]).

Changes in the kinetic energy of the body were described by the applied GRF acting on the centre of mass (COM) [11]. Nevertheless, the position of the COM relative to the line of action of the resultant GRF has not yet been taken into consideration when determining propulsion. It has even been shown in other human locomotion like running or walking [31] and also ski skating [32] that during the entire movement cycle, the resultant forces are hardly ever directed through the COM. Hence, besides the translatory effects (force directed through the COM) of the resultant forces, rotatory effects and external moments may also play a role. This raises the question of whether the produced ski and pole forces acting on the ground during skating movements exclusively accelerate the skier's COM forward and thus determine the forward speed of the skier during skating movements. How much of the applied force is capable of accelerating the COM forward has not yet been examined, and the question of whether skiers with the highest propulsive forces are also the fastest in any case may be of interest to better discriminate different performance levels in XC skiers.

For quantification of the separate contributions of the right and left legs and poles to the overall COM forward acceleration, the development of an extended methodology is suggested. It is proposed that applied GRFs be considered with respect to the position of the COM in space, meaning that the translatory share of the force pointing from the point of force application through the COM is derived. This goes beyond the identification of the propulsive share of GRFs as commonly used [15] and may allow determination of the forward acceleration of each skier's COM and the contribution of different leg and/or arm actions in XC skiing.

Accordingly, the main aims of the current study were to determine the COM acceleration by combining force and 3D motion capture data as well as to evaluate the proposed methodology through a comparison with the COM acceleration derived from 3D motion capture measurements. A secondary goal was to demonstrate the applicability of this methodology to a representative ski-skating technique involving both leg and pole thrusts.

## 2 Materials and methods

### 2.1 Experimental protocol, participants, and techniques

The experimental protocol and all methods used in this study were approved by the Ethics Committee of the University of Jyväskylä. All participants provided written informed consent prior to measurements and were free to withdraw from the experiments at any point. Nine highly skilled male XC skiers ( $32 \pm 7$  years;  $178 \pm 6$  cm;  $77 \pm 6$  kg;  $VO_{2max}$ :  $73 \pm 2$  ml/kg/min;  $116 \pm 56$  FIS points) volunteered and participated in this study. Measurements were carried out on a nearly flat (incline:  $1^\circ$ ) section of the Vuokatti ski tunnel (Finland), where the temperature and humidity were kept constant at  $-4^\circ\text{C}$  and 85%, respectively.

A technique of ski skating without poles (Fig. 1a) was chosen to show the appropriateness of the proposed methodology. During this skiing technique, the arm movements were restricted by supporting the hands at the hips such that propulsion was limited to the legs, while relative body movements through arm actions like swinging or positioning for poling were minimized. Thus, the comparableness to motion data was considered to be as high as possible.

Furthermore, as it is representative of skating techniques that combine pole and leg push-offs, V2-alternate (V2A) skating (Fig. 1b) was measured to exemplarily show the applicability of the developed methodology for a more complex skating mode using poles and legs. V2A is a very complex XC skiing technique [18] where one step is characterized by a leg push-off together with a double poling action. The second, subsequent step consists of a leg push-off accompanied by a dynamic double arm swing [33]. Together, both steps constitute one full V2A cycle (Fig. 1b). This technique was chosen because it is considered relevant to differentiate the contributions of leg push-offs and pole thrusts to overall acceleration in various skating techniques, for example to compare groups of skiers of different levels or the fatigued and non-fatigued states of an athlete. V2A data can only be presented for one representative participant of the group (36 years; 175 cm;

**Fig. 1** Serial pictures with selected key positions during **a** leg skating with restricted arm actions and **b** V2A skating technique with poles



73.4 kg;  $\text{VO}_2\text{max}$ : 75 ml/kg/min; 196 FIS points) due to technical problems with the pole force sensors during measurements.

Subjects performed three trials with maximal speed for leg skating ( $5.9 \pm 0.3$  m/s) and V2A ( $7.2 \pm 0.1$  m/s), respectively. All recorded skating strokes (one to two per trial) were analysed. One skating stroke was defined from the start to the end of ski-ground contact determined from the onset and offset of the vertical GRF (Fig. 2a; events 1'–3'). The gliding (Fig. 2a; event 1'–2') and push-off phases (Fig. 2a; event 2'–3') were separated by the minimum of vertical GRF (Fig. 2a; event 2').

## 2.2 Force measurements

The general goal was to measure all three components of GRFs acting at the skis directly and accurately in field conditions on snow. Vertical, medio-lateral (transverse to the ski), and anterior–posterior (along the ski) GRFs were considered beforehand as relevant input data to be measured (Fig. 2a–d). Due to problematic and limiting mechanical cross talk that produced less accurate anterior–posterior forces along the ski in earlier versions of a 3D force binding [34], two custom-made 2D force measurement bindings for XC skiing (Neuromuscular Research Centre, University of Jyväskylä, Finland) with a weight of 490 g each were built to measure GRFs at 1000 Hz. Force bindings were calibrated using special calibration devices and procedures [14]. One pair of prepared racing skis (Peltonen Supra-x, Peltonen Ski Oy, Hartola, Finland, 188 cm, 1170 g each) was used by all skiers. The left ski was equipped with binding 1 (Fig. 2b) to measure the vertical ( $F_3$ ) and medio-lateral ( $F_1$ ) forces, while binding 2 (Fig. 2c), which measured the vertical ( $F_3$ ) and anterior–posterior ( $F_2$ ) forces, was mounted on the right ski. The corresponding third force component on each side was, respectively, estimated as follows: for the left ski, the anterior–posterior forces ( $F_{2e}$ ) were derived from the

measured vertical forces ( $F_3$ ) by calculating frictional forces ( $F_e = \mu F_3$ ) using the mean coefficient of friction ( $\mu$ ) for each participant derived from all measured skating strokes on the contralateral side. As medio-lateral forces cannot be estimated, forces acting on the right ski ( $F_{1e}$ ) were equalized to the measured ones on the contralateral left side, and therefore those measured values were duplicated, oriented, and shifted by the duration of one skating stroke and thus coupled to the measured vertical and anterior–posterior forces at the right ski.

During V2A trials, GRFs at the poles were measured (1000 Hz) with a custom-made, lightweight (70 g each) pole force system (University of Salzburg, Austria). Uni-axial strain gauge load cells (Velomat, Kamenz, Germany) were installed in a specially constructed light aluminium body fitting into the pole grips (Fig. 3c) of selected racing poles adjusted to the preferred length of each skier. Calibration of the pole sensors was processed with standard procedures in accordance with previous studies [35–37]. The validity of the system was examined on an established force platform system (Neuromuscular Research Centre, University of Jyväskylä, Finland) [9]. The mean absolute resultant pole force deviation over ground contact was  $9.3 \pm 11.3$  N.

## 2.3 Three-dimensional motion capture

All skating techniques were analysed in 3D and recorded (100 Hz) by the Vicon Nexus motion capture system (Vicon, Oxford, UK) installed in the Vuokatti ski tunnel (Fig. 3a). The system consisted of 16 infrared cameras (T-Series T40S) mounted on a wooden frame on the side walls and ceiling of the tunnel and covered with special cold protectors (Fig. 3a). This setup enabled a measurement range of up to 18 m with full-body COM detection corresponding to one to three steps per trial depending on skiing speed. A setup of 51 passive reflective markers was used. Marker placement corresponded to the full-body plug-in

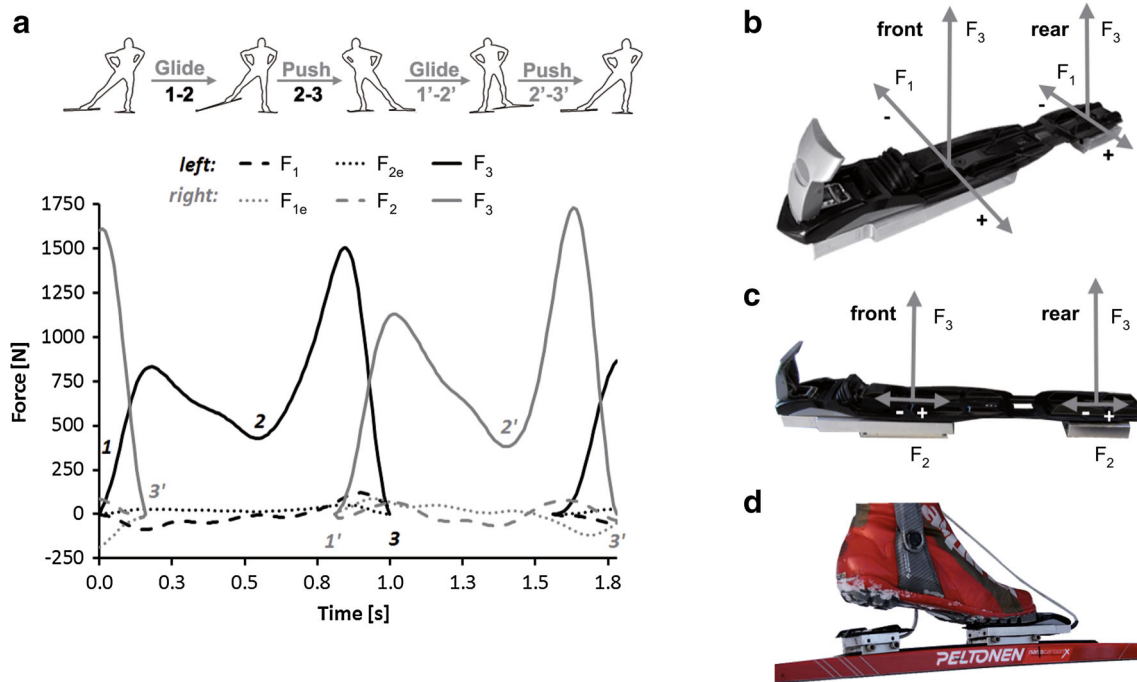


**Fig. 2 a** Representative curves of the directly measured medio-lateral ( $F_1$ ) and vertical ( $F_3$ ) forces on the left leg (black solid/broken lines) and anterior–posterior ( $F_2$ ) and vertical ( $F_3$ ) forces on the right leg (grey solid/broken lines), and the estimated anterior–posterior ( $F_{2e}$ ) (black dotted line) and medio-lateral ( $F_{1e}$ ) forces (grey dotted line) on the corresponding other side. Forces are sums of the respective forefoot and rear foot parts of the bindings. Numbers in the curves indicate the start (event 1) and end (event 3) of one leg's

ground contact during skating. Gliding (events 1–2) and push-off (events 2–3) phases are separated by the local force minimum (event 2) in all analysed ground reaction force curves. **b** Force binding 1, measuring the medio-lateral ( $\pm F_1$ ) and vertical ( $F_3$ ) force components, and **c** force binding 2, measuring the anterior–posterior ( $\pm F_2$ ) and vertical ( $F_3$ ) force components, in both cases measured separately by a front (f) and a rear (r) unit [35]. **d** System mounted on the racing ski

gait (PIG) setup [38] with three additional markers on each ski (Fig. 3b), two additional markers on each pole, and additional markers on both trochanter major, mid-sternum, and mid-spine.

Three-dimensional motion data from the trials were initially processed with Vicon Nexus 1.7.1 software (Vicon, Oxford, UK) using standard labelling and gap-filling procedures [38]. To determine the COM, the Vicon Nexus software includes the so-called PIG model, which has not been clinically tested [38]. Therefore, the accuracy of COM detection in body positions relevant for XC skiing had to be verified. Adaptations in the thorax and abdomen/pelvis segments were necessary and performed using a self-written cross-country skier body model (XC model), which was created using Body Language scripting in the Vicon Body Builder 3.6.1 (Vicon, Oxford, UK). The XC model was based on Dempster's body segment data as described by Winter [39]. To validate the XC model and to test the accuracy of the COM positions in space, two additional procedures were performed.

A skier performed several trials of a single leg stance with different body positions, considered to be relevant during ski skating, on an AMTI force plate (Advanced Mechanical Technology Inc., Watertown, USA) with a fully

installed PIG marker setup plus markers on the right and left trochanter major. The COM position was calculated using the PIG as well as the XC model. First, the validation of the horizontal COM position (anterior–posterior and medio-lateral) from the XC model and the comparison to PIG data were done by comparing the horizontal position of the COM projected onto the ground (COMP) with centre of pressure (COP) data from the AMTI force plate. The mean distance between COMP and COP was  $6.0 \pm 3.8$  mm for the XC model versus  $84.4 \pm 14.4$  mm for the PIG model. In a second step, the vertical COM position was detected with a custom gravity scale (University of Salzburg, Austria) used as a reference system to establish accuracy in this dimension. The skier lay supine on a long board. A prism rod was mounted at one end of the board and a gravity scale at the other end. From the displayed weight differences between the unloaded and loaded board, the height of the COM could be calculated. The COM position was obtained from the XC model and used for the respective body positions, showing a mean deviation from the gravity scale of  $-8.5 \pm 6.0$  mm, while the PIG model gave a deviation of  $-2.3 \pm 2.1$  mm. Skis and poles were added to the XC model as additional segments. After this model optimization process, COM was calculated from the motion capture



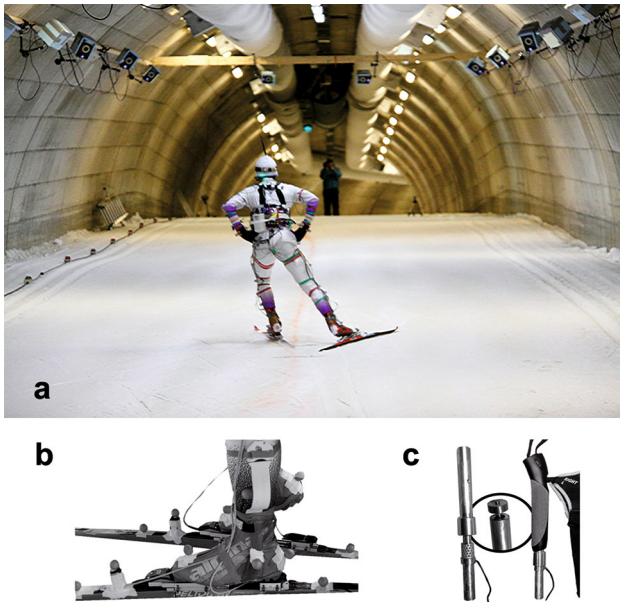


**Fig. 3** **a** Cross-country skier performing leg skating in the measurement area covered by the Vicon Nexus (Vicon, Oxford, UK) motion capture system with 16 infrared cameras installed in the Vuokatti ski tunnel (Finland). **b** Instrumented skis equipped with force bindings and reflective Vicon markers attached to the skis, boots, and lower legs. **c** Lightweight pole force system with uniaxial strain gauge load cells (Velomat, Kamenz, Germany) installed in an aluminium body and mounted in the pole grips

data using the Vicon Nexus software by running the PIG model from a pipeline including the standard Woltring (GCV) filter routine followed by the XC model.

## 2.4 Data collection

Signals from the force bindings and pole force system were transferred via cables to an eight-channel force amplifier (Neuromuscular Research Centre, University of Jyväskylä, Finland) linked to a National Instruments A/D converter card (sampling rate: 1 kHz; NI 9205) and a wireless transmitter system (WLS-9163, National Instruments, Austin, USA) that sent data to a portable computer with a receiver card and custom-made data collection software (Labview 8.5; National Instruments, Austin, USA). Three-dimensional motion data were collected and pre-processed with the Vicon Nexus 1.7.1 software (Vicon, Oxford, UK). Participants wore a custom-made waist pack (Fig. 3a) on the lower back with a total weight of 2590 g containing all the named measurement equipment. All pole and leg force systems were synchronized with a sync step prior to each skiing trial, producing peaks of the pole and leg forces, respectively. For the synchronization of force and motion data, an analogue trigger signal was simultaneously recorded by both data collection systems.

## 2.5 Centre of mass acceleration

### 2.5.1 Reference value

The marker-based motion capture system Vicon Nexus is considered a current standard in 3D kinematic analyses [40]. It allows an accurate determination of the skier's COM position from body segments' position data and makes it possible to determine the acceleration of COM [40]. To calculate the net force acting on the COM in a forward direction ( $F_m$ ), forward acceleration of the COM was multiplied by each participant's mass inclusive of equipment ( $m$ ) (Table 1). Hereafter, this variable served as the reference value.  $F_m$  shows how the athlete overcomes resistive forces (e.g. air drag and friction) and contains—like a black box—inseparable information on the contribution of all single pole and leg thrusts and relative movements of body segments. Thus, the extent to which each pole or leg thrust contributes to the acceleration of the skier's COM in the skiing direction cannot be obtained solely from kinematic 3D analyses. This is the reason why computation from GRFs is essential and it is proposed that it be combined with kinematic input data.

### 2.5.2 Transformation from the local to the global coordinate system

The first prerequisite for calculating the forces in the skiing direction is to express the pole and leg forces in the motion capture coordinate system. Three-dimensional forces derived from force binding measurements (Fig. 4 $F_1$ ,  $F_2$ ,  $F_3$ ) were transformed to a motion capture coordinate system by the rotational matrices

$$\begin{pmatrix} F_x \\ F_y \\ F_z \end{pmatrix} = (F_1 \quad F_2 \quad F_3) \begin{bmatrix} \cos(\beta) & 0 & \sin(\beta) \\ 0 & 1 & 0 \\ -\sin(\beta) & 0 & \cos(\beta) \end{bmatrix} \begin{bmatrix} 1 & 0 & 0 \\ 0 & \cos(\gamma) & \sin(\gamma) \\ 0 & -\sin(\gamma) & \cos(\gamma) \end{bmatrix} \begin{bmatrix} \cos(\alpha) & \sin(\alpha) & 0 \\ -\sin(\alpha) & \cos(\alpha) & 0 \\ 0 & 0 & 1 \end{bmatrix}, \quad (1)$$

using the YXZ Cardan ski angles ( $\alpha$  ski orientation towards Y;  $\beta$  ski edging;  $\gamma$  tilt of the skis) derived from motion analyses (Figs. 4, 5) [38].

From these force components, the magnitude of resultant force

$$F_r = \sqrt{F_x^2 + F_y^2 + F_z^2} \quad (2)$$

could be computed (Table 1).

To obtain the point of force application (PFA) in the motion capture coordinate system (Table 1), the ski origin

**Table 1** Descriptions of abbreviations and definitions

Abbreviation	Term	Descriptions and definitions <sup>a</sup>
COM	Centre of mass	Centre of mass calculated from 3D motion analyses and body model data
PFA	Point of force application	Point of force application along the ski binding calculated from force binding data and the position of the ski segment in space
$F_m$	Net force at COM from motion capture	Net force in skiing direction and acting at the COM determined from 3D motion capture data This corresponds to the forward acceleration multiplied by the mass of the subject plus equipment
$F_r$	Resultant force	Resultant force calculated from 2D ground reaction forces measured with force bindings and the estimated third dimension
$F_n$	Net force	Net force acting at the PFA determined from force calculation. This corresponds to the propulsive component of $F_r$ pointing in the skiing direction, acting at the PFA, and corrected for resistive forces
$F_t$	Translational force	Component of $F_r$ pointing from the PFA towards the COM
$F_{ro}$	Rotational force	Component of $F_r$ perpendicular to $F_t$ , inducing a moment about the COM
$F_c$	Net force at COM calculated from force and motion capture data	Net force in the skiing direction and acting at the COM determined with the proposed methodology This corresponds to the component of $F_t$ pointing in the skiing direction, corrected for resistive forces and acting at the COM

<sup>a</sup> See also Fig. 7

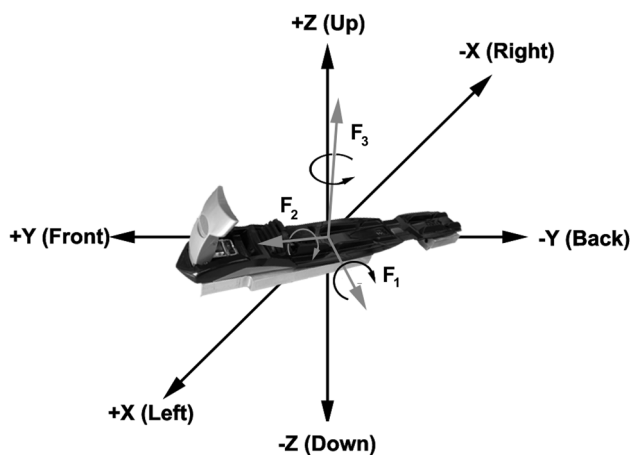


**Fig. 4** The motion capture coordinate system (black arrows) and the local coordinate system (grey arrows) showing the components of binding forces are defined as follows:  $F_1$  (medio-lateral),  $F_2$  (anterior-posterior), and  $F_3$  (vertical) with respect to the ski/binding. Coordinate transformation from the local binding to the motion capture coordinate system, correcting for orientation, edging, and tilt of the ski/binding by rotation around the vertical, anterior-posterior, and medio-lateral axes

was created as a virtual marker at the top of the force binding. Displacement of the PFA along the binding was calculated from the force distribution between the front and rear plates of the force binding in the ski system over time and was transferred to the motion capture coordinate system by moving the ski origin backwards along the ski by that value.

The measured axial pole forces were considered to be the resultant pole forces acting along the pole from the top of the pole to the pole tip and are therefore expressed that way in the motion capture coordinate system. The PFA for the pole was set at the pole tip, which was calculated as a virtual marker using pole length measures and position data of the pole markers.

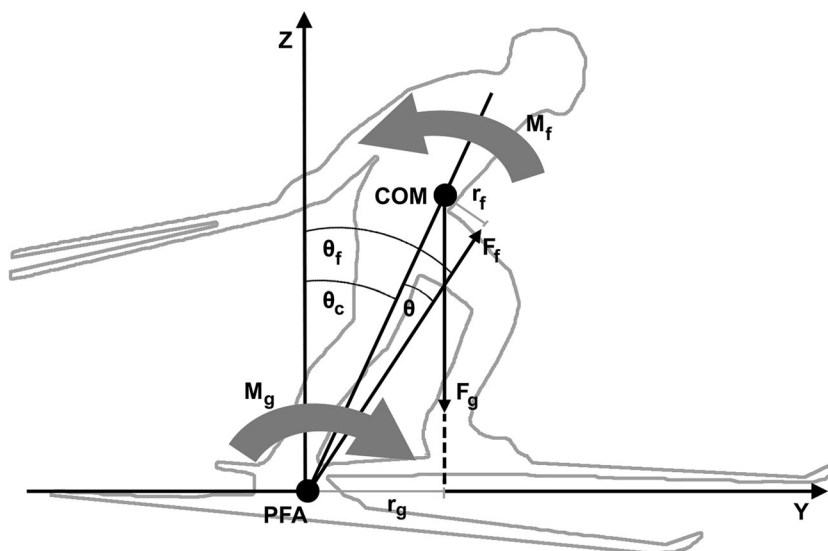
### 2.5.3 Net forces

A common approach to the quantification of propulsive forces ( $F_y$ ) is to quantify the component of  $F_r$  pointing in the desired skiing direction (e.g. [6, 11, 15, 16]). To be able to examine whether these calculated forces determine the acceleration of the skier in accordance with the described reference, the value of  $F_m$  should be checked, bearing in mind that  $F_m$  (Table 1) shows how the athlete was able to overcome resistive forces. For that reason, estimations of the resistive forces acting in each respective direction were included to determine the net forces ( $F_n$ ) (Table 1). As the skier was skiing slightly ( $1^\circ$ ) uphill, the track inclination ( $\delta$ ) was considered by expressing forces in the global coordinate system and determining

$$F_{g1} = F_y \cos(\delta) - F_z \sin(\delta). \quad (3)$$

Due to its line of action, gravity does not influence the component of  $F_{g1}$  in the desired skiing direction. Ski friction was calculated ( $F_{fr} = \mu F_3$ ) and is directed along the path of ski motion. Net forces were found from

**Fig. 5** Total angular momentum of the skier's body in the global sagittal plane (ZY) is based on the influence of gravitational ( $F_g$ ) and ground reaction forces ( $F_f$ ).  $F_g$  causes an external moment ( $M_g = r_g F_g$ ) about the point of force application (PFA) if the centre of mass (COM) deviates from the vertical position above PFA by an angle  $\theta_c$  ( $r_g$  and  $\theta_c > 0$ ). A deviation of the direction of  $F_f$  from the PFA–COM direction ( $\theta \neq 0$ ) induces an external moment ( $M_f = r_f F_f$ ) about the COM



$$F_n = F_{g1} - F_{fr} - F_d, \quad (4)$$

where the shares of ski friction along the skiing direction ( $F_{fr}$ ) and air drag ( $F_d$ ) were subtracted from  $F_{g1}$ . Air drag has been estimated with a mean value of 20 N [41] for the skiing speed of  $21.6 \pm 1.2$  km/h.

#### 2.5.4 Translational and rotational force components and whole body angular momentum

In running, Kugler and Janshen [31] showed that despite wanting to keep the whole body angular momentum small to maintain postural stability in a dynamic situation, faster athletes showed more forward leaning of the body during accelerated running. This means that moments caused by gravity ( $M_g$ ) must be compensated for by moments in the opposite direction, for example, by GRF passing the COM [31] in an anterior direction. This was also found in pre-measurements for the current ski-skating study (Figs. 5, 6b) and based on findings of earlier studies showing that skiers lean forward slightly during leg push-off [18] and the resultant GRF is not always directed through the COM over the entire skating cycle [32]. During leg push-off, the athlete leaned forward and GRF was almost never directed through the COM (Figs. 5, 6a).  $M_g$  was largely compensated for by moments induced by GRF ( $M_f$ ), and net moments ( $M_n$ ) were small (Fig. 6b) during leg push-off. Thus, despite external moments, the athlete did not rotate about PFA or COM, keeping the dynamic balance. At the end of push-off, net moments become greater (Fig. 6b), possibly to facilitate the positioning on the new gliding leg, which makes ground contact at this point in time.

Against the above-described background, it is likely that not all of the applied forces have direct effects on the

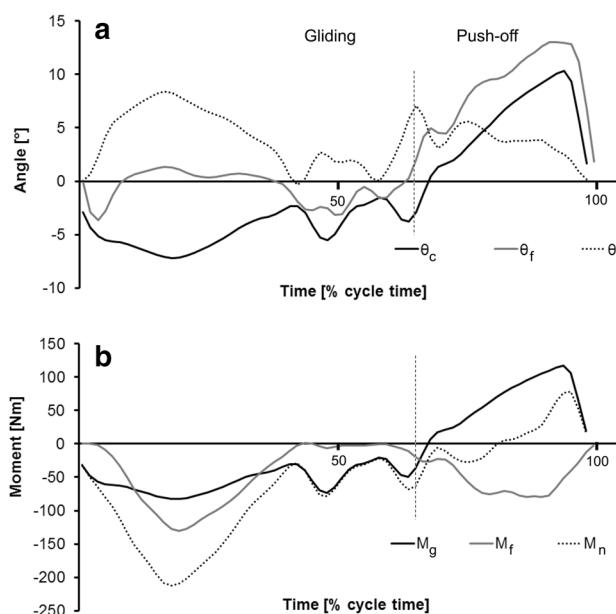
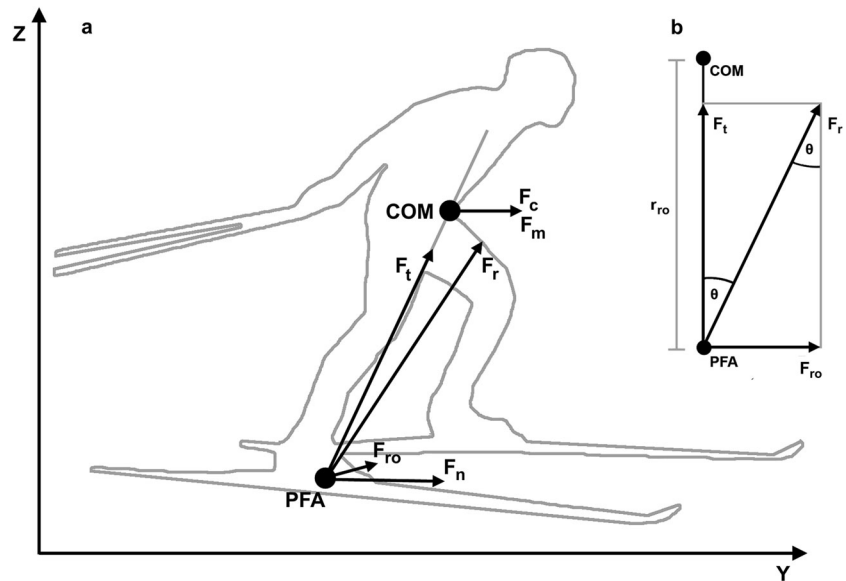


**Fig. 6** Representative time courses during one ski-ground contact (left leg; gliding plus push-off) during leg skating: **a** Forward lean angle ( $\theta_c$ ), angle of the resultant ground reaction force ( $F_f$ ) vector ( $\theta_f$ ), and the angle between the  $F_f$  vector and the PFA–COM direction ( $\theta$ ) all with respect to the vertical axis (Z) in the sagittal plane (Fig. 5); **b** External moments in the skiing direction induced by gravity ( $M_g$ ) and ground reaction force (left leg) ( $M_f$ ) as well as the remaining net moment ( $M_n$ )

translational movement of the skier represented by his COM. With respect to the skier's body, an applied force can rather have translational and/or rotational effects (Fig. 7). To quantify both effects,  $F_r$  was decomposed into two components (Fig. 7b). The translational force ( $F_t$ ) is the component of  $F_r$  acting in the direction from PFA to COM and is calculated from

**Fig. 7** **a** Illustration of measured and calculated forces acting at the point of force application (PFA) and the centre of mass (COM) of a skier. Definitions of all force components are shown in Table 1. **b** Illustration of the resultant ground reaction force  $F_r$  and its components for  $\theta \neq 0$ :  $F_t$  the translational force component through the COM; and  $F_{ro}$  the rotational force component perpendicular to  $F_t$  inducing a moment about the COM ( $M_f = r_{ro}F_{ro}$ )



$$F_t = \frac{F_r \cdot \mathbf{v}}{|\mathbf{v}|}, \quad (5)$$

where  $\mathbf{v}$  is the vector determined by PFA and COM. The rotational force component was derived from

$$F_{ro} = F_r - F_t, \quad (6)$$

where  $F_{ro}$  acts normal to  $F_t$  (Table 1; Fig. 7b) and induces a moment about the COM (Figs. 5 and 6b), the same amount as  $F_r$  does.

$F_c$  (Table 1) is the component of translational force pointing in the skiing direction (y). This force component induces the forward acceleration of the COM. Incline, ski friction, and air drag have been considered in the same manner as previously described for  $F_n$  (Formulae 3 and 4).

In V2A trials, the contribution of applied pole forces to COM acceleration ( $F_p$ ) was calculated analogously as previously described for the leg forces without considering possible slight pole bending when loaded.

Finally, the magnitude of all computed forces in the desired skiing direction were compared to the magnitude of  $F_m$ , the defined reference data from motion capture, and the forces are presented in values relative to body weight (%BW). For all forces ( $F_m$ ;  $F_c$ ;  $F_n$ ), the average and maximal values (%BW) as well as the mean, maximum, and minimum differences between  $F_m$  and  $F_c$  and between  $F_m$  and  $F_n$ , respectively, were calculated during the push-off and gliding phase.

## 2.6 Data processing and statistical analyses

Data processing was conducted using IKE-master 1.38 (IKE Software Solutions, Salzburg, Austria) including a 6-Hz fourth-order zero-lag low-pass Butterworth filter of

COM acceleration from motion data. Using IBM SPSS Statistics 20 (IBM Corporation, New York, USA), the differences between the determined forces on the COM were checked by  $t$  tests for normally distributed data. In the other cases, a Wilcoxon  $u$  test was carried out. To determine the correlation between time series, similarity coefficients (SCs), mathematically based on the Taylor polynomials [42, 43] between time-normalized force curves, were calculated using MATLAB (MathWorks, Natick, USA). Each SC was classified as follows:  $-1 < \text{similarity} < 1$ , where  $-1$  means contrary time histories,  $0$  means no similarity, and  $1$  means congruent time histories.

## 3 Results and discussion

### 3.1 Centre of mass acceleration determined from leg force and motion capture data

During the push-off phase, the average and maximum  $F_c$  did not differ from the used reference value  $F_m$  (Table 2) and the corresponding force–time curves showed a high match with an SC of 0.92 (Table 3; Fig. 8). During the gliding phase (Table 2), the average  $F_c$  was lower ( $P < 0.05$ ) with a mean difference of  $-7.2 \pm 2.9\%BW$  versus  $F_m$  (Table 3), while the force curves still demonstrated high similarity (Table 3; Fig. 8).

These results confirm the appropriateness of the assumptions made and the methodology developed for the push-off phase during leg skating. By combining binding force data and COM data from 3D motion capture, COM acceleration in the skiing direction can be quantified. This determination of  $F_c$  allows for the assessment of performance differences between athletes and, uniquely to this



**Table 2** Comparison of (1) net forces in the skiing direction acting at the COM determined from motion capture ( $F_m$ ), (2) net forces in the skiing direction acting at the COM derived with the proposed methodology ( $F_c$ ), and (3) net forces acting at the PFA at the ski ( $F_n$ ) during the leg push-off and gliding phases

Phase	Force (%BW)	$F_m$	$F_c$	$F_n$
Push-off	Average	$2.3 \pm 1.8$	$0.5 \pm 2.9$	$19.8 \pm 5.7a$
	Maximum	$13.1 \pm 3.3$	$14.3 \pm 4.8$	$35.2 \pm 6.1a$
Gliding	Average	$0.1 \pm 1.2$	$-6.9 \pm 2.7^a$	$12.2 \pm 2.5a$

Values are mean  $\pm$  SD;  $n = 9$

$P < 0.05$

<sup>a</sup> Different from  $F_m$

methodology, the contribution of right and left leg push-offs to the skier's forward acceleration can be estimated.

The difference in average force between  $F_c$  and  $F_m$  during the gliding phase shows that prediction of the acceleration of COM as derived from motion analyses is not fully possible with the introduced methodology. Thereby, the presented data cannot reveal whether the

difference between  $F_c$  and  $F_m$  in the gliding phase is due to a possibly limited validity of the methodology for deriving  $F_c$  or based on the characteristics of the reference value ( $F_m$ ). Considering the composition of  $F_m$  and  $F_c$  and the movement in the gliding phase, the latter appears to be more likely. The calculated value of  $F_c$  describes how much of the GRFs directly accelerate the skier's COM forward and at the respective point in time without indicating other effects. In comparison,  $F_m$ , as derived from motion capture data, equally contains this information, but additionally shows simultaneous impacts of posture and transfer/conservation of momentum. Relative movements such as arm swing and positioning (e.g. for poling) affect the reaction forces [44–46], the position of the COM, the posture of the body [47–50], and thus the body's inertia characteristics. In the present study, the reaction forces and position of the COM have been detected continuously over time and likewise included in the methodology to derive  $F_c$ . The changes in inertia characteristics have not been taken into account for  $F_c$ . Also, the possible influences of conservation of momentum (e.g. from a previous leg push-off) or aspects of momentum transfer (e.g. from arm to

**Table 3** Comparison of similarity coefficients (SCs) and mean, maximum, and minimum absolute differences computed over force curves between  $F_m$  and  $F_c$  and between  $F_m$  and  $F_n$

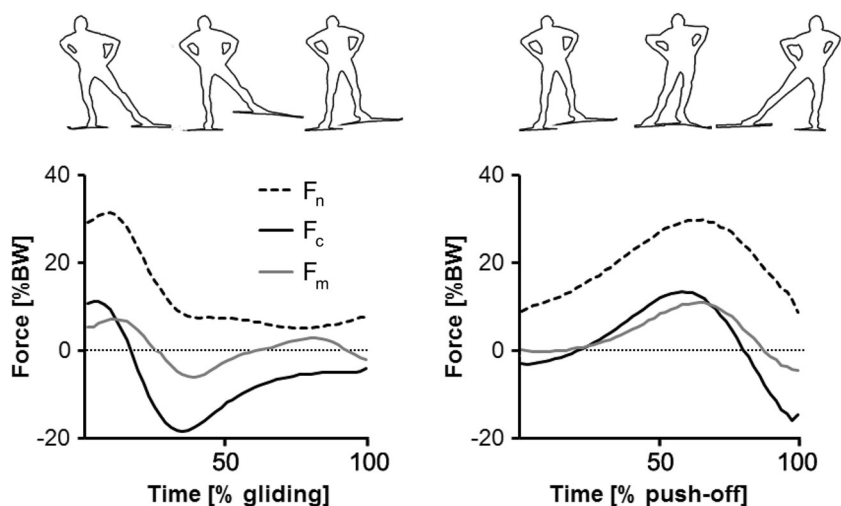
Phase	Comparison	Similarity coefficient SC	Differences (%BW)		
			Diff <sub>mean</sub>	Diff <sub>max</sub>	Diff <sub>min</sub>
Push-off	$F_m-F_c$	0.93	$-1.4 \pm 2.5$	$4.8 \pm 3.5$	$-13.0 \pm 6.0$
	$F_m-F_n$	0.92	$16.5 \pm 3.6^a$	$25.0 \pm 2.7^a$	$5.2 \pm 6.2^a$
Gliding	$F_m-F_c$	0.90	$-7.2 \pm 2.9$	$6.7 \pm 6.8$	$-17.4 \pm 6.9$
	$F_m-F_n$	0.70	$11.4 \pm 3.1^a$	$29.1 \pm 6.5^a$	$-0.8 \pm 5.4^a$

The range of SC is  $-1 < \text{similarity} < 1$ , where  $-1$  means contrary time histories,  $0$  means no similarity, and  $1$  means congruent time histories. Differences (%BW) are mean  $\pm$  SD;  $n = 9$

$P < 0.05$

<sup>a</sup> Different from  $F_m-F_c$

**Fig. 8** Time courses of the net force in the skiing direction acting at the COM and determined from motion capture ( $F_m$ ), net force in the skiing direction acting at the COM and calculated from the proposed model using combined force and motion capture data ( $F_c$ ), and net force (in the skiing direction) acting at the point of force application at the ski ( $F_n$ ). For definitions, see Table 1. Values are means during the gliding and push-off phases.  $n = 9$



body, when braking the arms after an active arm swing) have not been quantified [49, 50]. If these effects occur, the comparableness of  $F_c$  and  $F_m$  is reduced.

An exact reproduction of  $F_m$  was not the aim of the study. Therefore, a skating movement with reduced differentiating aspects was selected to compare  $F_c$  and  $F_m$ , and the movement of pure leg skating with restricted arm actions was deliberately chosen. Thereby, during the relevant push-off phase, a close fit of the  $F_c$  and  $F_m$  curves could be reached. During the gliding phase, the differences (Tables 2, 3) in average force values, which showed stronger braking effects with  $F_c$  (Fig. 8), may be partly explained by unavoidable relative movements of body segments. During one-legged gliding, the leg that performed the preceding push-off gets adducted and the body moves into a more upright position, moving the COM forward and upward in preparation for the following leg push-off [18]. This means that the angular momentum preserved from the prior push-off acts on the body whose position and inertial properties are changing during the gliding phase. This can by nature only be seen from the  $F_m$  values and not from the  $F_c$  values. In general,  $F_c$  is a relevant parameter to describe the output during push-off in an applied skiing technique.  $F_c$  during the gliding phase can be determined, but has to be interpreted in the context previously shown.

Commonly used measurement systems and literature-based estimations (air resistance, friction) are not perfect. They do, however, demonstrate small but acceptable limitations (e.g. [14, 35, 41]). Advances in measurement systems (e.g. 3D binding) may contribute to a more accurate determination in the future [14].

The methodology to derive  $F_c$  allows expanded analyses of each athlete's skiing techniques. Additionally,  $F_c$ , calculated as a percentage of overall applied GRFs, could be used as a kind of effectiveness index for push-off motions, like the one already used for propulsive forces [15]. Principally,  $F_c$  can be calculated for all push-off actions during a ski-skating cycle, showing how much the right or left leg and/or pole contributes to the COM forward acceleration and how these sources of COM forward acceleration change between different performance levels, techniques, speeds, track inclinations, or selected equipment like ski, boot, or pole systems. Additionally, computing the differences between  $F_c$  and  $F_m$  may help to filter out which other technique aspects besides the push-offs performed (e.g. the conservation of momentum) accelerate or decelerate the COM in the desired skiing direction at specific points of time during the ski-skating cycle. This highlights the necessity of both  $F_c$  as well as  $F_m$  for technique analysis in elite sports, knowing that both are strongly related but not necessarily equivalent in value.  $F_c$  can be used to isolate and quantify the role and effectiveness of the leg push-offs.

In principle, the same methodology can be applied to leg push-offs in classical skiing techniques like diagonal stride or double poling with kick.

### 3.2 Net leg forces

During the push-off phase, the average and maximum values of  $F_n$  were approximately ninefold and threefold higher ( $P < 0.05$ ) than  $F_m$  (Table 2), respectively, although the shapes of the  $F_n$  and  $F_m$  curves were similar, demonstrating an SC of 0.92 (Table 3; Fig. 8). Likewise for the gliding phase, overrating of  $F_n$  ( $P < 0.05$ ) could be observed (Table 2), while the similarity of the  $F_n$  time course dropped to an SC of 0.70 (Table 3; Fig. 8). Supporting these results, the mean differences for the  $F_m$  time courses were greater ( $P < 0.05$ ) for  $F_n$ , with overestimates of approximately 11 and 17%BW (86 and 125 N) for the gliding and push-off phases, respectively, whereas  $F_c$  indicates a slight underestimation (-7 to -1%BW) (Table 3). Focusing on two examples of skiers showing almost the same maximum and average values of  $F_n$  (Fig. 9a), the difference between their  $F_c$  values was found to be as high as 5.1% in the most extreme cases (Fig. 9b).

This latter finding becomes very important when analysing the techniques of two skiers or two trials of one athlete. Comparing  $F_n$  may lead to the same ratings for either athletes or trials; however, the quality of leg push-offs and their effects on the forward acceleration of the COM could be quite different.  $F_c$  may thus offer additional information and technique diagnostics in elite sports. With that, athletes may benefit from the specific technique criterion provided by  $F_c$ . Nevertheless, the fact that the shapes of  $F_n$  and  $F_m$  curves were similar indicates that the principal structure of leg push-offs can be obtained from  $F_n$ . This is relevant in coaching and technique feedback training sessions when a laborious detection of the COM is not possible and if, for example, the effectiveness of push-offs [15] is needed for comparison purposes.

In contrast to  $F_c$ ,  $F_n$  overestimated the forward acceleration of the skier, which can also be looked at from a mechanical perspective. The overestimate found in the current study means that the resultant push-off force  $F_r$  was rarely directed from the PFA through the COM (Figs. 5, 6a) during leg skating, which has also been shown for other XC skiing techniques [32]. Thus, a considerable part of  $F_r$  did not help to accelerate the COM in the desired skiing direction, and whole body angular momentum around the COM was induced (Figs. 5, 6a, b). The latter could functionally add to maintaining the dynamic balance during skating push-offs by compensating moments caused by gravity and the COM position (Fig. 5). This has also been found in other human locomotion modes like accelerated running [31, 51]. The small remaining net moments

**Fig. 9** Time courses of the **a** net forces acting at the points of force application ( $F_n$ ) and **b** net forces in the skiing direction acting at the COM and calculated from the proposed model ( $F_c$ ) for two participants (S1 and S2)

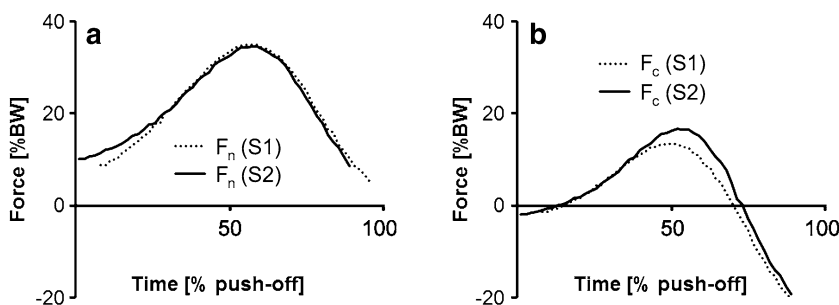


(Fig. 6b) at the end of the leg push-off may contribute to changing the body position with respect to the PFA. This may facilitate the positioning of the COM over the PFA of the new gliding ski (weight transfer), which gets ground contact during the final phase of the contralateral leg’s push-off (Fig. 1a, b).

### 3.3 Contribution of legs and poles to acceleration in V2A skating

$F_c$  was derived from the data of one representative top athlete performing the V2A technique (Fig. 1b) to provide an example of the applicability of the proposed methodology in skating techniques that combine pole and leg thrusts. The observation of a full V2A cycle (Fig. 10) resulted in an SC of 0.75 between  $F_m$  and  $F_c$ , which was slightly lower than the values from leg skating only that were used with the whole of the investigated group ( $>0.90$ ) and a single athlete ( $>0.91$ ). In the poling phase (Fig. 10, poling), the average  $F_c$  including data from poles and legs was  $9.9 \pm 2.7\%BW$ , while the reference value  $F_m$  was  $10.5 \pm 1.1\%BW$ . The maximum values in the respective phase for  $F_m$  and  $F_c$  reached  $23.3 \pm 0.4$  and

$25.0 \pm 7.8\%BW$ . During pole and leg thrusts within one full V2A cycle, the impulse of  $F_c$  was 35.2 Ns from poles and 18.2 Ns from legs. This indicates that the contribution of the poles (65.9%) to the total forward acceleration of the COM during V2A-skating was clearly greater than that of the legs (35.1%) (Fig. 10).

The data and findings indicate that COM acceleration can be calculated from combined leg and pole forces, even in a complex technique, and the contributions of the legs and poles can be determined separately. The absolute value and contribution of poles to COM acceleration ( $F_p$ ) should be carefully considered, as poles were assumed to be stiff in the current study, revealing a certain limitation of this application. Pole bending will occur to a certain extent [52]. Systems measuring the axial pole forces at the grip have been widely used to collect force data [35]. Thus, detailed studies should be performed to control the influence of pole bending on the production of propulsion, the forces applied, and the calibration process performed.

The differences between  $F_m$  and  $F_c$  were greater for V2A compared to leg skating with restricted arm movements and are therefore most likely dependent on the skiing technique used. Compared to leg skating, V2A is a technique with considerably more relative movements due to the described arm and leg movements and vertical movement of the COM. Relative movement may lower the comparableness to the reference value  $F_m$  (see also Chapter 3.1). The V2A technique is thus not convenient for evaluating the methodology, but is useful for showing its applicability.

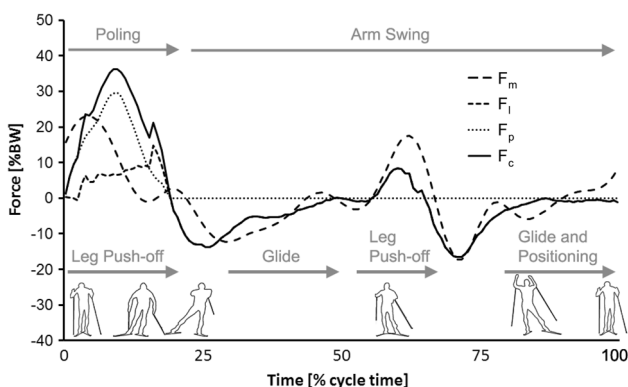


**Fig. 10** Time courses over a full V2A-skating cycle of the net force in the skiing direction acting at the COM and determined from motion capture ( $F_m$ ) (broken line), determined from force and motion capture data ( $F_c$ ) (solid line). The net pole forces ( $F_p$ ) (dotted line) and net leg force ( $F_l$ ) (short broken line), both in the skiing direction, contributing independently to the COM acceleration, are illustrated separately. Values are means of two V2A-skating cycles

## 4 Conclusions

The comparison of the proposed methodology to the reference value from motion capture measurements showed no differences during push-offs in leg skating, revealing that it is appropriate to quantify a skier’s forward acceleration during this phase by considering GRFs with respect to the COM position. In contrast to the determination of COM acceleration from motion data alone, it becomes feasible to detect and separate the sources of acceleration

during XC skiing. The determination of the COM acceleration from GRF data alone gives force–time curves of comparable shape, but leads to a considerable overestimation of the COM acceleration compared to motion data. Thus, ski and pole forces are not always directed towards the COM and do not exclusively serve to accelerate the athlete, but may play an important role in regulating dynamic balance. Consideration of the COM position relative to the line of action of GRFs during leg skating turned out to be an essential factor when aiming to quantify the athletes' acceleration. In V2A, the contribution of poles and legs to the acceleration of the skier could be calculated, providing an example and a perspective for XC skiing techniques using propelling leg and pole thrusts.

The proposed methodology may offer new possibilities for diagnosing the biomechanics of skiing techniques. It enables to compare skiers with varying levels of performance and/or techniques and to evaluate the influence of speed, incline, or equipment. Potentially, this methodology may be employed to investigate the influence of edging and ski angle during skating or to quantify the influence of resistive forces, such as the role of body weight, drag, or altered friction. The full applicability of the proposed methodology to different XC skating and classical techniques with poles needs to be further investigated and developed through follow-up studies.

**Acknowledgements** Open access funding provided by Paris Lodron University of Salzburg. The authors would like to thank Prof. David Bacharach from St. Cloud University (USA) for valuable comments on the manuscript and language optimization, and Jürgen Pfusterschmied and laboratory engineer Teemu Heikkinen for assistance with technological challenges before and during the study. We want to thank Falk Göpfert for valuable work on automation processes in data processing and the participating staff and athletes for their enthusiasm and effort during the study.

#### Compliance with ethical standards

**Conflicts of interest** The authors declare that they have no conflicts of interest.

**Open Access** This article is distributed under the terms of the Creative Commons Attribution 4.0 International License (<http://creativecommons.org/licenses/by/4.0/>), which permits unrestricted use, distribution, and reproduction in any medium, provided you give appropriate credit to the original author(s) and the source, provide a link to the Creative Commons license, and indicate if changes were made.

#### References

- Kent M (2006) Oxford dictionary of sports science and medicine. Oxford University Press, New York
- Saibene F, Minetti AE (2003) Biomechanical and physiological aspects of legged locomotion in humans. *Eur J Appl Physiol* 88(4/5):297–316. doi:10.1007/s00421-002-0654-9
- Formenti F, Ardigò LP, Minetti AE (2005) Human locomotion on snow: determinants of economy and speed of skiing across the ages. *Proc R Soc B: Biol Sci* 272(1572):1561–1569. doi:10.1098/rspb.2005.3121
- Rusko H (2008) Handbook of sports medicine and science, cross country skiing. Blackwell Science, Oxford. doi:10.1002/9780470693834.index
- Stöggl T, Lindinger S, Müller E (2007) Analysis of a simulated sprint competition in classical cross country skiing. *Scand J Med Sci Spor* 17(4):362–372. doi:10.1111/j.1600-0838.2006.00589.x
- Smith GA (1992) Biomechanical analysis of cross-country skiing techniques. *Med Sci Sport Exerc* 24(9):1015–1022
- Komi PV (1987) Force measurements during cross-country skiing. *Int J Sport Biomech* 3:370–381
- Ekström H (1981) Force interplay in cross-country skiing. *Scand J Sports Sci* 3(3):69–76
- Vähäsöyrinki P, Komi PV, Seppälä S, Ishikawa M, Kolehmainen V, Salmi JA, Linnamo V (2008) Effect of skiing speed on ski and pole forces in cross-country skiing. *Med Sci Sport Exerc* 40(6):1111–1116. doi:10.1249/MSS.0b013e3181666a88
- Leppävuori AP, Karras M, Rusko H, Viitasalo JT (1993) A new method of measuring 3-D ground reaction forces under the ski during skiing on snow. *J Appl Biomech* 9(4):315–328
- Hoset M, Rognstad A, Rølvåg T, Ettema G, Sandbakk Ø (2014) Construction of an instrumented roller ski and validation of three-dimensional forces in the skating technique. *Sports Eng* 17(1):23–32. doi:10.1007/s12283-013-0130-2
- Lindinger S (2007) Biomechanics in cross-country skiing – methods and future research questions. In: Linnamo V, Komi P, Müller E (eds) *Science and Nordic Skiing—Proc 1st Int Congr Science and Nordic Skiing (ICSNS)*. Meyer & Meyer Sport, Oxford, pp 23–42
- Lindinger SJ, Komi P, Ohtonen O, Linnamo V (2013) Developments and methodological aspects in cross-country skiing research. In: Hakkarainen A, Linnamo V, Lindinger SJ (eds) *Science and Nordic Skiing II – Proc 2nd Int Congr Science and Nordic Skiing (ICSNS)*. University of Jyväskylä, Jyväskylä, pp 13–22
- Ohtonen O, Lindinger S, Lemmettylä T, Seppälä S, Linnamo V (2013) Validation of portable 2D force binding systems for cross-country skiing. *Sports Eng* 16(4):281–296. doi:10.1007/s12283-013-0136-9
- Stöggl T, Holmberg H-C (2014) Three-dimensional force and kinematic interactions in V1 skating at high speeds. *Med Sci Sport Exer* 47(6):1232–1242
- Street GM, Frederick EC (1995) Measurement of skier-generated forces during roller-ski skating. *J Appl Biomech* 11:245–245
- Andersson E, Stöggl T, Pellegrini B, Sandbakk Ø, Ettema G, Holmberg H-C (2012) Biomechanical analysis of the herringbone technique as employed by elite cross-country skiers. *Scand J Med Sci Sports* 24(3):542–552. doi:10.1111/sms.12026
- Lindinger S (2006) *Biomechanische Analysen von Skatingtechniken im Skilanglauf*. Meyer & Meyer, Aachen
- Stöggl T, Müller E, Lindinger S (2008) Biomechanical comparison of the double-push technique and the conventional skate skiing technique in cross-country sprint skiing. *J Sport Sci* 26(11):1225–1233. doi:10.1080/02640410802027386
- Stöggl T, Kampel W, Müller E, Lindinger S (2010) Double-push skating versus V2 and V1 skating on uphill terrain in cross-country skiing. *Med Sci Sport Exerc* 42(1):187–196
- Mikkola J, Laaksonen MS, Holmberg H-C, Nummela A, Linnamo V (2013) Changes in performance and poling kinetics during cross-country sprint skiing competition using the double-poling technique. *Sport Biomech* 12(4):355–364. doi:10.1080/14763141.2013.784798



22. Zory R, Vuillerme N, Pellegrini B, Schena F, Rouard A (2009) Effect of fatigue on double pole kinematics in sprint cross-country skiing. *Hum Mov Sci* 28(1):85–98. doi:[10.1016/j.humov.2008.05.002](https://doi.org/10.1016/j.humov.2008.05.002)
23. Bilodeau B, Boulay MR, Roy B (1992) Propulsive and gliding phases in four cross-country skiing techniques. *Med Sci Sport Exerc* 24(8):917–925
24. Lindinger SJ, Stöggl T, Müller E, Holmberg H-C (2009) Control of speed during the double poling technique performed by elite cross-country skiers. *Med Sci Sport Exerc* 41(1):210–220. doi:[10.1249/MSS.0b013e318184f436](https://doi.org/10.1249/MSS.0b013e318184f436)
25. Göpfert C, Holmberg H-C, Stöggl T, Müller E, Lindinger SJ (2013) Biomechanical characteristics and speed adaptation during kick double poling on roller skis in elite cross-country skiers. *Sport Biomech* 12(2):154–174. doi:[10.1080/14763141.2012.749939](https://doi.org/10.1080/14763141.2012.749939)
26. Linnamo V, Ohtonen O, Rapp W, Lemmettylä T, Göpfert C, Komi P, Ishikawa M, Holmberg H, Vähäsöyrinki P, Mikkola J (2013) Sports technology, science and coaching. In: Hakkarainen A, Lindinger SJ, Linnamo V (eds) 2nd Int Congr Science and Nordic Skiing (ICSNS), Vuokatti, 2012
27. Stöggl T, Lindinger S (2007) Double-push skating and klap-skate in cross-country skiing, technical developments for the future? In: Schwameder H, Strutzenberger G, Fastenbauer V, Lindinger S, Müller E (eds) 24th Int Symp Biomechanics in Sports (2006), Salzburg. ISBS-Conf Proc Arch. doi:[10.1249/MSS.0b013e3181ac9748](https://doi.org/10.1249/MSS.0b013e3181ac9748)
28. Stöggl T, Müller E, Ainegren M, Holmberg H-C (2011) General strength and kinetics: fundamental to sprinting faster in cross country skiing? *Scand J Med Sci Sports* 21(6):791–803. doi:[10.1111/j.1600-0838.2009.01078.x](https://doi.org/10.1111/j.1600-0838.2009.01078.x)
29. Swarén M, Therell M, Eriksson A, Holmberg H-C (2013) Cross-country ski poles: introduction of a shaft strength index. In: Hakkarainen A, Lindinger SJ, Linnamo V (eds) Proc 2nd Int Congr Science and Nordic Skiing (ICSNS), Vuokatti, 2012
30. Ohtonen O, Lindinger S, Linnamo V (2013) Effects of gliding properties of cross-country skis on the force production during skating technique in elite cross-country skiers. *Int J Sports Sci Coach* 8(2):407–416. doi:[10.1260/1747-9541.8.2.407](https://doi.org/10.1260/1747-9541.8.2.407)
31. Kugler F, Janshen L (2010) Body position determines propulsive forces in accelerated running. *J Biomech* 43(2):343–348
32. Clauß M-S (2011) Biomechanische Explikationen zu den Skating-Skilanglauftechniken. [Biomechanical explications of the skating cross-country skiing techniques]. Dissertation, Leipzig University, Leipzig
33. Smith GA (2008) Cross-country skiing: technique, equipment and environmental factors affecting performance. In: Zatsiorsky V (ed) *Biomechanics in Sport*. Blackwell Science, pp 247–270. doi:[10.1002/9780470693797.ch12](https://doi.org/10.1002/9780470693797.ch12)
34. Linnamo V, Ohtonen O, Stöggl T, Komi P, Müller E, Lindinger S (2012) Multi-dimensional force measurement binding used during skating in cross-country skiing. In: Müller E, Lindinger S, Stöggl T (eds) *Science and Skiing V*. pp 540–548
35. Ohtonen O, Lindinger S, Lemmettylä T, Seppälä S, Linnamo V (2013) Validation of portable 2D force binding systems for cross-country skiing. *Sports Eng* 16(4):281–296. doi:[10.1007/s12283-013-0136-9](https://doi.org/10.1007/s12283-013-0136-9)
36. Holmberg H-C, Lindinger S, Stöggl T, Eitzlmair E, Müller E (2005) Biomechanical analysis of double poling in elite cross-country skiers. *Med Sci Sport Exerc* 37(5):807–818. doi:[10.1249/01.mss.0000162615.47763.c8](https://doi.org/10.1249/01.mss.0000162615.47763.c8)
37. Lindinger SJ, Holmberg H-C (2011) How do elite cross-country skiers adapt to different double poling frequencies at low to high speeds? *Eur J Appl Physiol* 111(6):1103–1119. doi:[10.1007/s00421-010-1736-8](https://doi.org/10.1007/s00421-010-1736-8)
38. Stöggl T, Lindinger S, Müller E (2006) Biomechanical validation of a specific upper body training and testing drill in cross-country skiing. *Sport Biomech* 5(1):23–46
39. Vicon-Motion-Systems (2007) Plug in gait model details
40. Winter DA (2009) *Biomechanics and motor control of human movement*. John Wiley & Sons, New Jersey. doi:[10.1002/9780470549148.index](https://doi.org/10.1002/9780470549148.index)
41. Chardonens J, Favre J, Le Callennec B, Cuendet F, Gremion G, Aminian K (2012) Automatic measurement of key ski jumping phases and temporal events with a wearable system. *J Sport Sci* 30(1):53–61. doi:[10.1080/02640414.2011.624538](https://doi.org/10.1080/02640414.2011.624538)
42. Svensson E (1994) *Ski Skating with Champions: “How to ski with [the] least energy”*. Ski Skating with Champions, Seattle
43. Birklbauer J (2006) *Modelle der Motorik: eine vergleichende Analyse moderner Kontroll-, Steuerungs- und Lernkonzepte*. Meyer & Meyer, Aachen
44. Nakazato K, Scheiber P, Müller E (2011) A comparison of ground reaction forces determined by portable force-plate and pressure-insole systems in alpine skiing. *J Sport Sci Med* 10(4):754
45. Ashby BM, Heegaard JH (2002) Role of arm motion in the standing long jump. *J Biomech* 35(12):1631–1637
46. Hegge AM, Etema G, de Koning JJ, Rognstad AB, Hoset M, Sandbakk Ø (2014) The effects of the arm swing on biomechanical and physiological aspects of roller ski skating. *Hum Mov Sci* 36:1–11. doi:[10.1016/j.humov.2014.05.001](https://doi.org/10.1016/j.humov.2014.05.001)
47. Göpfert C, Lindinger SJ, Ohtonen O, Rapp W, Müller E, Linnamo V (2016) The effect of swinging the arms on muscle activation and production of leg force during ski skating at different skiing speeds. *Hum Mov Sci* 47:209–219. doi:[10.1016/j.humov.2016.03.009](https://doi.org/10.1016/j.humov.2016.03.009)
48. King D (2001) Generation of vertical velocity in toe-pick figure skating jumps. *Biomechanics Symposia (2001)*, University of San Francisco. ISBS-Conf Proc Arch
49. Feltner ME, Fraschetti DJ, Crisp RJ (1999) Upper extremity augmentation of lower extremity kinetics during countermovement vertical jumps. *J Sports Sci* 17:449–466
50. Harman EA, Rosenstein MT, Frykman PN, Rosenstein RM (1990) The effects of arms and countermovement on vertical jumping. *Med Sci Sports Exerc* 22(6):825–833
51. Cheng KB, Wang CH, Chen HC, Wu CD, Chiu HT (2008) The mechanisms that enable arm motion to enhance vertical jump performance – A simulation study. *J Biomech* 41(9):1847–1854
52. Hay JG, Wilson BD, Dapena J, Woodworth GG (1977) A computational technique to determine the angular momentum of a human body. *J Biomech* 10(4):269–277